# Long-Duration Gamma-Ray Flares and Solar Energetic Particles

**A. Bruno**[1,2], S. Dalla[3], G.A. de Nolfo[1], A. Hutchinson[1,4], T. Laitinen[3], I.G. Richardson[1,5], J.M. Ryan[6]

[1] NASA Goddard Space Flight Center
[2] Catholic University of America
[3] Jeremiah Horrocks Institute, University of Central Lancashire
[4] University of Maryland, Baltimore
[5] University of Maryland, College Park
[6] Space Science Center, University of New Hampshire

11th International Fermi Symposium
09/12/2024

# Long-Duration Gamma-Ray Flares

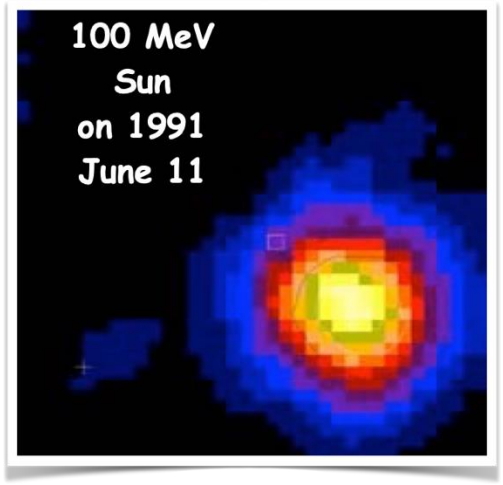


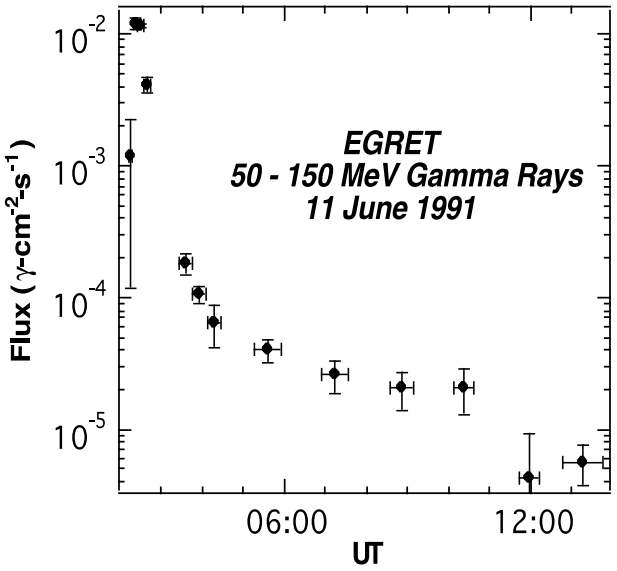


- ✓High-energy (>50 MeV up to several GeV) γ-ray emission first reported in the 1980s by the *Solar Maximum Mission* and the *Compton Gamma Ray Observatory*.
- ✓Spectrum consistent with the decay of neutral pions produced in the interactions of ≳300 MeV protons and ≳200 MeV/n $\alpha$ particles with the Sun chromosphere and photosphere (high-density regions).
- ✓Delayed (minutes to hours) and extended (up to tens of hours) component after the impulsive phase, not accompanied by other flare-related emissions (e.g., X-rays, UV); harder ion spectrum.
- ✓Lack of temporal structures on scales much less than the overall decay time suggesting ion acceleration taking place over large volumes (≳$10^5$ km), smoothing over the details of the dynamics.

# Long-Duration Gamma-Ray Flares

- The high-energy delayed/extended emission was called "*long-duration gamma-ray flares" (Kanbach et al., 1993; Akimov et al., 1996; Ryan, 2000).*

☞ **Extended source distinct from impulsive flare.**

Two conflicting requirements (Ming Zhang, priv. comm.):

1) *we must contain the particles in a large volume over a long enough time to accelerate them without losing them;*
2) *and once they are lost from that acceleration volume, there must be numerous, efficient and reliable routes for them to precipitate to the Sun.*

# Two Competing Scenarios

## LDGRFs → continued particle acceleration or gradual interaction of trapped particles

Back-precipitation of particles accelerated in coronal mass ejection (CME)-driven shocks, i.e. the dominant mechanism for gradual solar energetic particle (SEP) events measured in situ; also referred to as *late-phase gamma-ray emission*

(*Wild et al. 1963; Ramaty et al. 1987; Cliver et al. 1993; Kocharov et al. 2015; Pesce-Rollins et al. 2015, 2022; Plotnikov et al. 2017; Gopalswamy et al. 2018, 2020; Jin et al. 2018; Kahler et al. 2018; Kouloumvakos et al. 2020*)

Particle trapping with/without continuous acceleration within large (≳1 Rs) coronal loops, characterized by a delayed onset representing the time required by the ions to exceed the pion production threshold energy

(*Ryan & Lee 1991; Mandzhavidze & Ramaty 1992; Chupp & Ryan 2009; Grechnev et al. 2018; de Nolfo et al. 2019; Ryan et al. 2019; de Nolfo et al. 2021*)

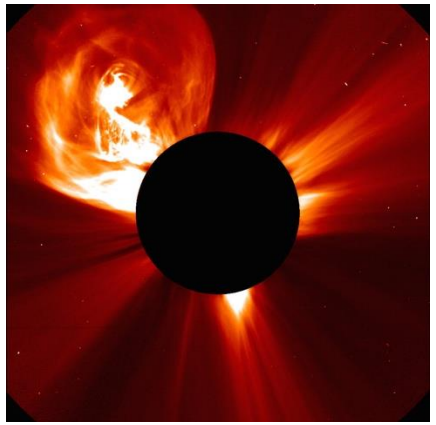

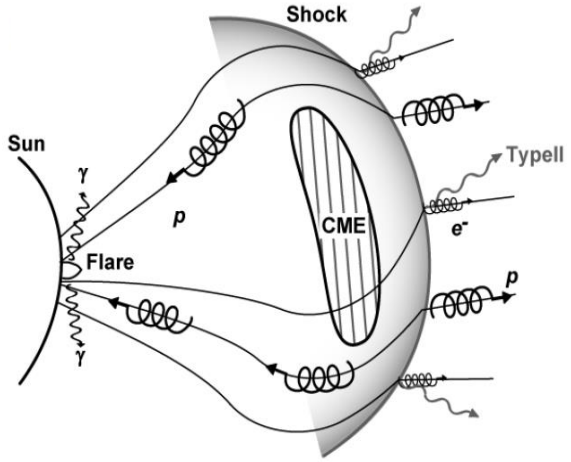


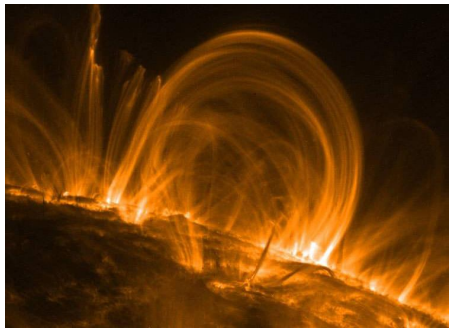

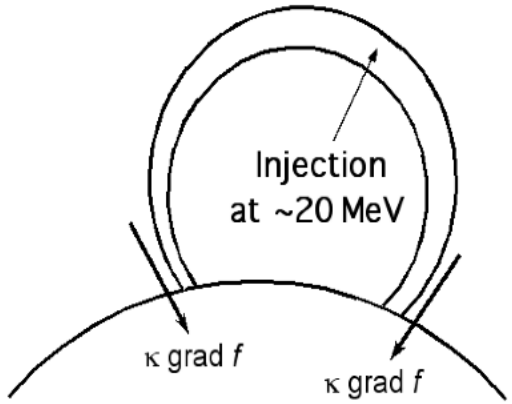


Protons obey spatial and momentum diffusion (2nd order Fermi)

$$\frac{\partial f}{\partial t} = \frac{1}{p^2}\frac{\partial}{\partial p}\left(p^2 D \frac{\partial f}{\partial p}\right) + \frac{\partial}{\partial x}\left(\kappa \frac{\partial f}{\partial x}\right) + Q$$

***⇒ both models have supporting observations***

# *Fermi*-LAT observations of LDGRFs

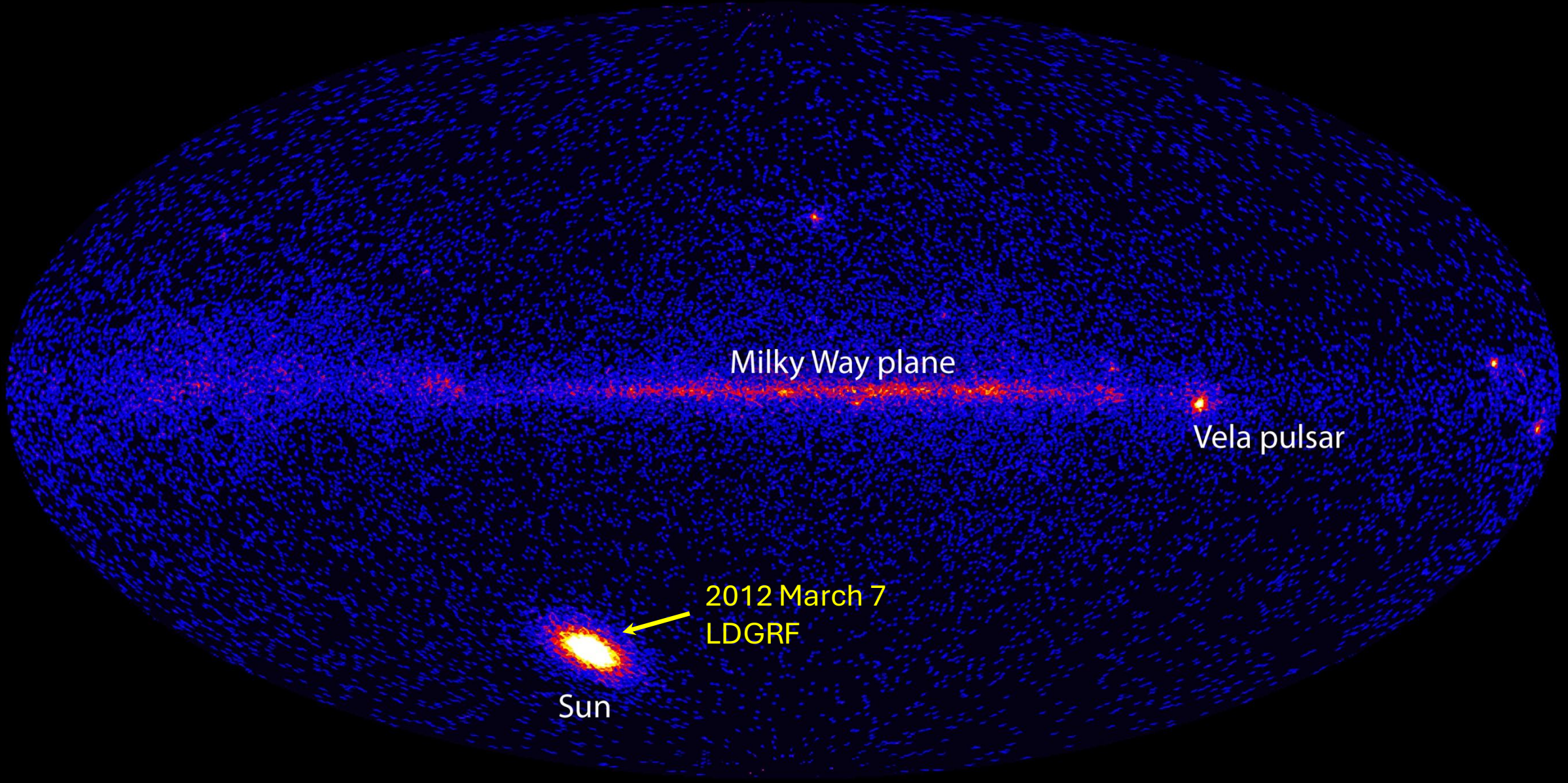

# *Fermi*-LAT Observations of LDGRFs

- Significant increase in the number (and accuracy) of solar γ-ray event observations wrt previous experiments
- Monitoring of solar eruptions over cycles 24 and 25
- Sun typically observed for ~20-40 min every 1-2 orbits for an averaged duty cycle of 15%-20%
- In response to a “burst” trigger from GBM during a high-energy flare, Fermi can autonomously be pointed at the Sun for up to 5 hours
- In addition, when the Sun is in an unusually high state of activity, a target of opportunity can be declared
- The high spatial resolution enables the localization of the centroid of the γ-ray emission on the solar atmosphere (for brightest eruptions)

# *Fermi*-LAT Observations of LDGRFs

Number of important constraints added to a growing picture; major improvement in the understanding of such phenomena (see, e.g., *Share et al. 2018*) :

- >100 MeV emission more common than previously thought, even with moderate flares
- Spectra consistent with the production from the decay of neutral pions
- Impulsive phase followed by a temporally distinct, extended phase with smooth exponential decay
- More (x10) fluence in delayed than impulsive phase
- Somewhat spatially extended emission
- Typical association with CMEs, type-II IP radio emission and SEP events, similar timescales
- Not necessarily linked to strong soft X-ray flares, but correlated with hard X-ray emission >100 keV

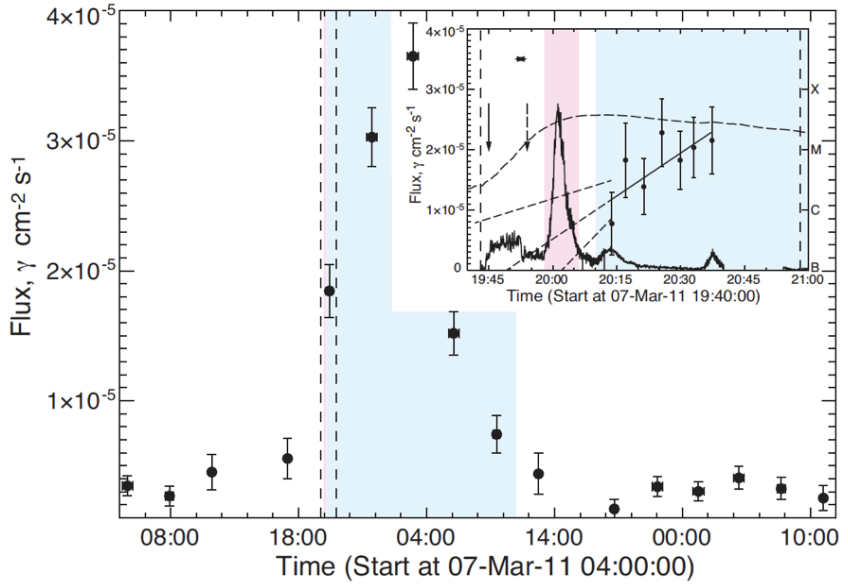


**Time history of > 100 MeV gamma-ray flux from Fermi/LAT. Inset compares with GBM 100-300 keV & dashed curve is soft x-rays**

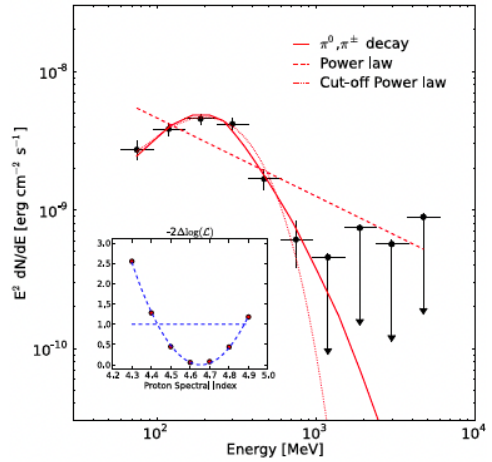

# *Fermi*-LAT Solar Flare Catalog

- 45 total events with emission in the γ-ray energy band 30 MeV – 10 GeV (≥5$\sigma$ significance) detected between 2010-2018.
- Light curves, spectra, proton indices, localizations, and estimates of the number of >500 MeV protons producing the LDGRFs
- 37 flares with delayed emission after the prompt-impulsive HXR phase; >2 hrs duration for 57% of them
- 3 behind-the-limb flares
- Rich and diverse sample of events with a wide variety of characteristics

FLSF Catalog for Flares Detected with the Fermi-LAT `SunMonitor` and Their Likely GOES X-Ray Flare Associations

| Name | GOES Class | GOES Start–Stop | Detection duration (hr) | Total Duration (hr) | Peak Flux ($10^{-5}$ cm$^{-2}$ s$^{-1}$) | Fluence >100 MeV (cm$^{-2}$) | Flare Type | Total Protons >500 MeV ($10^{27}$) |
|---|---|---|---|---|---|---|---|---|
| FLSF 2011 Mar 7 | M3.7[c] | 19:43–20:58 | 13.5 | 15.8 ± 3.1 | 3.23 ± 0.22 | 1.076 ± 0.029 | Delayed | 64.4 ± 1.8 |
| FLSF 2011 Jun 7 | M2.5 | 06:16–06:59 | 3.8 | 6.0 ± 2.2 | 3.18 ± 0.20 | 0.295 ± 0.030 | Delayed | 19.5 ± 2.0 |
| FLSF 2011 Aug 4 | M9.3 | 03:41–04:04 | 0.7 | 2.3 ± 0.7 | 2.30 ± 0.18 | 0.13 ± 0.05 | Delayed | 9 ± 4 |
| FLSF 2011 Aug 9 | X6.9 | 07:48–08:08 | 0.5 | 0.87 ± 0.34 | 2.29 ± 0.23 | 0.037 ± 0.018 | Prompt Short-Delayed[a] | 2.7 ± 1.3 |
| FLSF 2011 Sep 6 | X2.1 | 22:12–22:24 | 0.6 | 2.0 ± 1.4 | 22.8 ± 0.4 | 0.87 ± 0.17 | LLE-Prompt Short-Delayed[a] | 58 ± 12 |
| FLSF 2011 Sep 7 | X1.8 | 22:32–22:44 | 0.8 | 2.02 ± 0.35 | 0.77 ± 0.08 | 0.041 ± 0.014 | Delayed | 2.3 ± 0.7 |
| FLSF 2011 Sep 24 | X1.9 | 09:21–09:48 | 0.5 | 1.2 ± 0.7 | 0.50 ± 0.10 | 0.014 ± 0.007 | LLE-Prompt Short-Delayed[a] | ... |
| FLSF 2012 Jan 23 | M8.7 | 03:38–04:34 | 5.3 | 5.9 ± 1.0 | 1.99 ± 0.12 | 0.340 ± 0.014 | Delayed | 24.7 ± 1.0 |
| FLSF 2012 Jan 27 | X1.7 | 17:37–18:56 | 5.3 | 6.8 ± 1.5 | 3.3 ± 0.5 | 0.248 ± 0.025 | Delayed | 17.2 ± 1.8 |
| FLSF 2012 Mar 5 | X1.1 | 02:30–04:43 | 3.8 | 4.4 ± 1.2 | 0.63 ± 0.07 | 0.085 ± 0.007 | Delayed | 6.1 ± 0.5 |
| FLSF 2012 Mar 7 | X5.4[c] | 00:02–00:40 | 19.6 | 20.3 ± 0.8 | 233 ± 8 | 33.996 ± 0.030 | Delayed | 1844.7 ± 1.3 |
| FLSF 2012 Mar 9 | M6.3 | 03:22–04:18 | 5.5 | 7.2 ± 1.7 | 0.96 ± 0.12 | 0.148 ± 0.007 | No-Prompt Delayed | 9.29 ± 0.23 |
| FLSF 2012 Mar 10 | M8.4 | 17:15–18:30 | 2.3 | 6 ± 4 | 0.23 ± 0.06 | 0.042 ± 0.012 | Delayed | 2.3 ± 0.6 |
| FLSF 2012 May 17 | M5.1 | 01:25–02:14 | 2.1 | 2.6 ± 0.5 | 1.19 ± 0.19 | 0.0572 ± 0.0026 | Delayed | 2.29 ± 0.09 |
| FLSF 2012 Jun 3 | M3.3 | 17:48–17:57 | 0.4 | 1.9 ± 1.5 | 3.06 ± 0.25 | 0.117 ± 0.031 | LLE-Prompt Short-Delayed[a] | 7.7 ± 2.0 |
| FLSF 2012 Jul 6 | X1.1 | 23:01–23:14 | 0.8 | 1.27 ± 0.35 | 3.06 ± 0.15 | 0.100 ± 0.021 | Delayed | 7.5 ± 1.6 |
| FLSF 2012 Oct 23 | X1.8 | 03:13–03:21 | 0.5 | 1.9 ± 0.5 | 0.73 ± 0.18 | 0.047 ± 0.018 | LLE-Prompt Delayed[a] | ... |
| FLSF 2012 Nov 13 | M6.0 | 01:58–02:04 | 0.7 | 0.041 ± 0.006 | 0.46 ± 0.09 | 0.006 ± 0.022 | Prompt | ... |
| FLSF 2012 Nov 27 | M1.6 | 15:52–16:03 | 0.8 | 0.166 ± 0.025 | 0.27 ± 0.07 | 0.005 ± 0.030 | Prompt Short-Delayed | ... |
| FLSF 2013 Apr 11 | M6.5 | 06:55–07:29 | 0.7 | 0.38 ± 0.27 | 5.71 ± 0.24 | 0.099 ± 0.016 | No-Prompt Short-Delayed | 6 ± 6 |
| FLSF 2013 May 13a | X1.7 | 01:53–02:32 | 0.7 | 4.0 ± 1.3 | 0.96 ± 0.11 | 0.11 ± 0.06 | Delayed | 8 ± 5 |
| FLSF 2013 May 13b | X2.8 | 15:48–16:16 | 3.9 | 6.1 ± 2.2 | 2.41 ± 0.21 | 0.35 ± 0.04 | Delayed | 19.7 ± 2.3 |
| FLSF 2013 May 14 | X3.2 | 00:00–01:20 | 5.6 | 5.9 ± 0.5 | 3.30 ± 0.15 | 0.401 ± 0.004 | No-Prompt Delayed | 27.82 ± 0.28 |
| FLSF 2013 May 15 | X1.2 | 01:25–01:58 | 0.8 | 3.5 ± 0.5 | 0.36 ± 0.07 | 0.052 ± 0.023 | No-Prompt Delayed | ... |
| FLSF 2013 Oct 11 | M4.9* | 07:01–07:45 | 0.7 | 0.38 ± 0.32 | 12.5 ± 0.4 | 0.262 ± 0.013 | BTL Short-Delayed | 9 ± 9 |
| FLSF 2013 Oct 25a | X1.7 | 07:53–08:09 | 0.7 | 1.4 ± 0.5 | 1.15 ± 0.12 | 0.042 ± 0.013 | Delayed | 3.3 ± 1.0 |
| FLSF 2013 Oct 28 c | M2.7[c] | 14:46–15:04 | 0.3 | 1.6 ± 0.6 | 0.81 ± 0.12 | 0.036 ± 0.014 | Delayed | ... |
| FLSF 2014 Jan 06 | X3.5* | 07:40–08:08 | 0.6 | 0.27 ± 0.04 | 0.42 ± 0.09 | 0.0061 ± 0.0028 | BTL Short-Delayed | 0.31 ± 0.31 |
| FLSF 2014 Jan 07 | X1.2 | 18:04–18:58 | 0.8 | 1.05 ± 0.26 | 0.29 ± 0.07 | 0.0081 ± 0.0020 | Delayed | ... |
| FLSF 2014 February 25 | X4.9 | 00:39–01:03 | 6.7 | 8.4 ± 1.8 | 169.6 ± 2.0 | 13.95 ± 0.18 | LLE-Prompt Delayed[a] | 719 ± 8 |
| FLSF 2014 Jun 10 | X1.5 | 12:36–13:03 | 0.4 | 1.9 ± 0.6 | 1.17 ± 0.26 | 0.064 ± 0.026 | LLE-Prompt Delayed[a] | ... |
| FLSF 2014 Jun 11 | X1.0 | 08:59–09:10 | 0.4 | 0.23 ± 0.17 | 0.99 ± 0.26 | 0.007 ± 0.005 | Short-Delayed | ... |
| FLSF 2014 Sep 1 | X2.4* | 10:58–11:40 | 1.9 | 2.5 ± 1.2 | 379 ± 7 | 12.1 ± 2.3 | BTL Delayed | (7.4 ± 1.4) × $10^2$ |
| FLSF 2014 Sep 10 | X1.6 | 17:21–18:20 | 0.3 | 0.30 ± 0.06 | 7.4 ± 0.5 | 0.172 ± 0.012 | Short-Delayed | 5 ± 5 |
| FLSF 2015 Jun 21 | M2.7[c] | 02:04–03:15 | 10.1 | 11.5 ± 2.5 | 1.26 ± 0.15 | 0.296 ± 0.011 | Prompt Delayed | 16.7 ± 0.7 |
| FLSF 2015 Jun 25 | M7.9 | 08:02–09:05 | 0.7 | 2.4 ± 1.3 | 0.40 ± 0.08 | 0.030 ± 0.004 | Delayed | 2.28 ± 0.29 |
| FLSF 2017 Sep 6a | X2.2 | 08:57–09:17 | 0.5 | 0.169 ± 0.025 | 1.31 ± 0.16 | 0.020 ± 0.007 | Prompt | 0.6 ± 0.6 |
| FLSF 2017 Sep 6b | X9.3[c] | 11:53–12:10 | 13.0 | 13.33 ± 0.32 | 3.6 ± 0.5 | 1.0700 ± 0.0022 | Delayed | 79.41 ± 0.13 |
| FLSF 2017 Sep 10 | X8.2 | 15:35–16:31 | 13.3 | 13.9 ± 1.2 | 291.0 ± 2.1 | 22.2 ± 1.6 | Prompt Delayed[a] | (9.5 ± 0.7) × $10^2$ |

**Note.** In the GOES-class column, entries with an * identify the BTL flares, whose class is estimated based on the STEREO observation, and [a] indicates that there is also an LLE detection of the flare. The analysis results for the LLE flares are shown in Table 3.

# The 2012 March 7 LDGRF

- Exceptional in brightness and duration (>20 hours) (*Ajello et al. 2014).*
- Associated with X5.4 and X1.3 flares from same AR 11429 (N16E29) peaking one hr apart (00:24 UT & 01:14 UT), and very fast (3146 and 2160 km/s) CMEs.
- First eruption responsible for most SEPs in space (*e.g., Richardson et al. 2014*).
- One short LDGRF followed by a much longer LDGRF *(Share et al., 2018)*
- The fluxes and spectra of the γ rays evolve differently during the two LDGRFs.
- The SEP spectral index is similar to the one inferred for the interacting protons in the first LDGRF, but lower than the one associated with the second LDGRF.

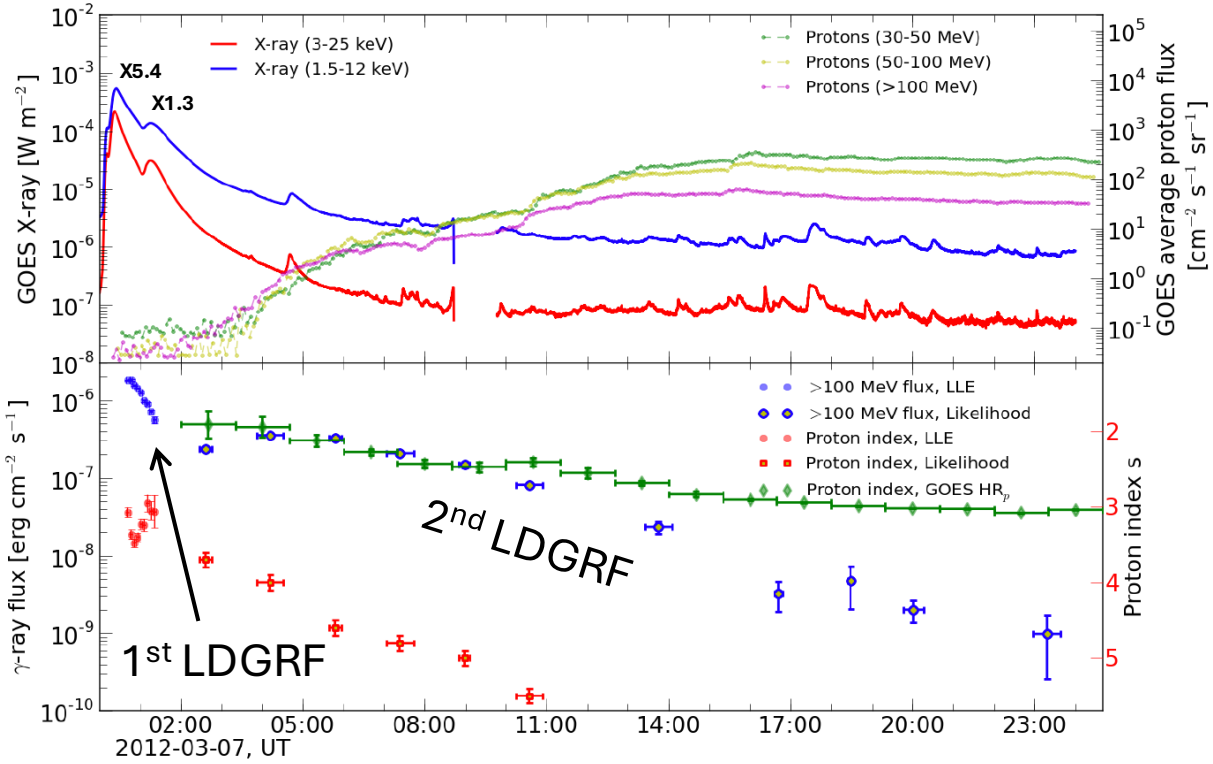


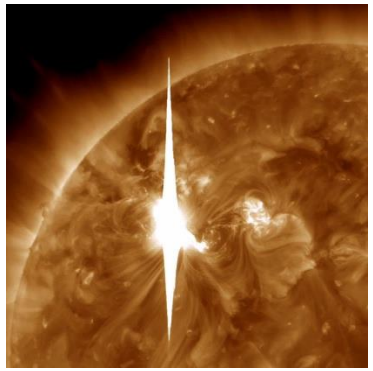

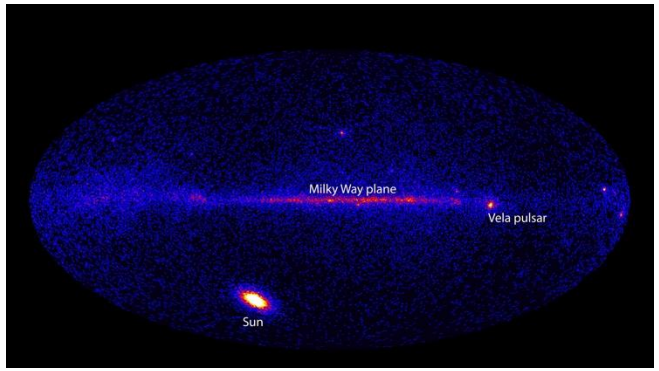

# The 2012 March 7 LDGRF

- The centroid of the emission was consistent with the flare location to within 10$^{o}$
- Some evidence of a progressive movement of the source across the solar disk over several hrs.
- First event for which this movement has been observed, interpreted as supporting evidence for the CME-shock scenario.
- The displacement at later times might be due to a larger dispersion of particles due to the longer distance traveled from the shock.
- However, as discussed later, the CME travelled ~80 Rs in 10hr, making questionable an efficient back-precipitation of shock-accelerated particles.

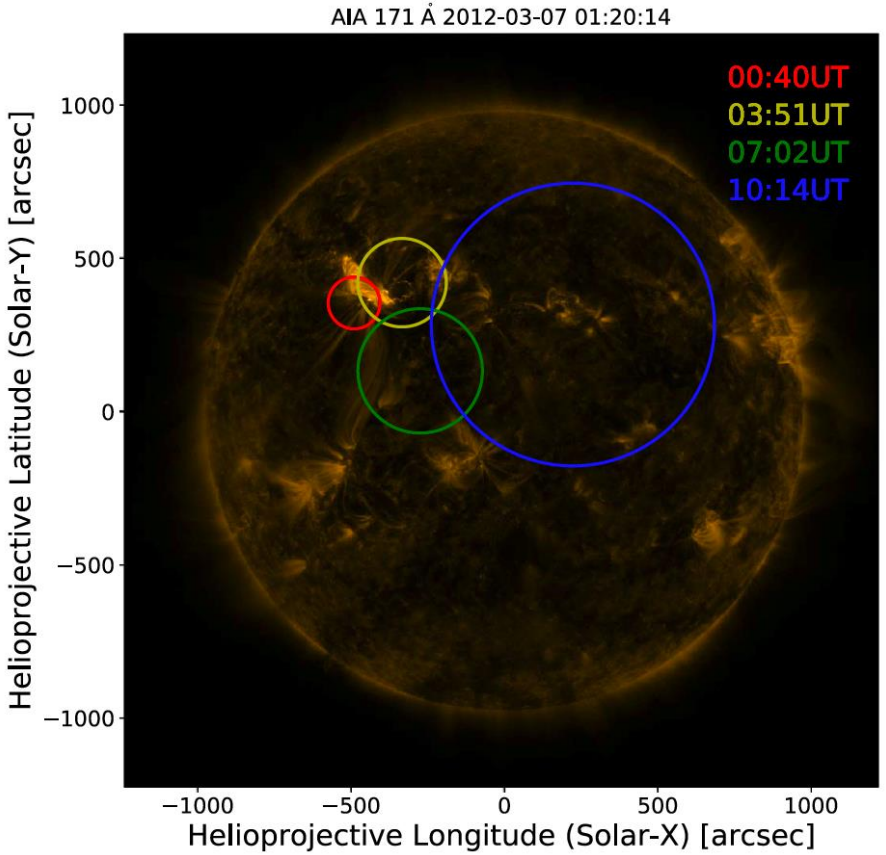


*error radii at 95% confidence*

# The 2012 March 7 LDGRF

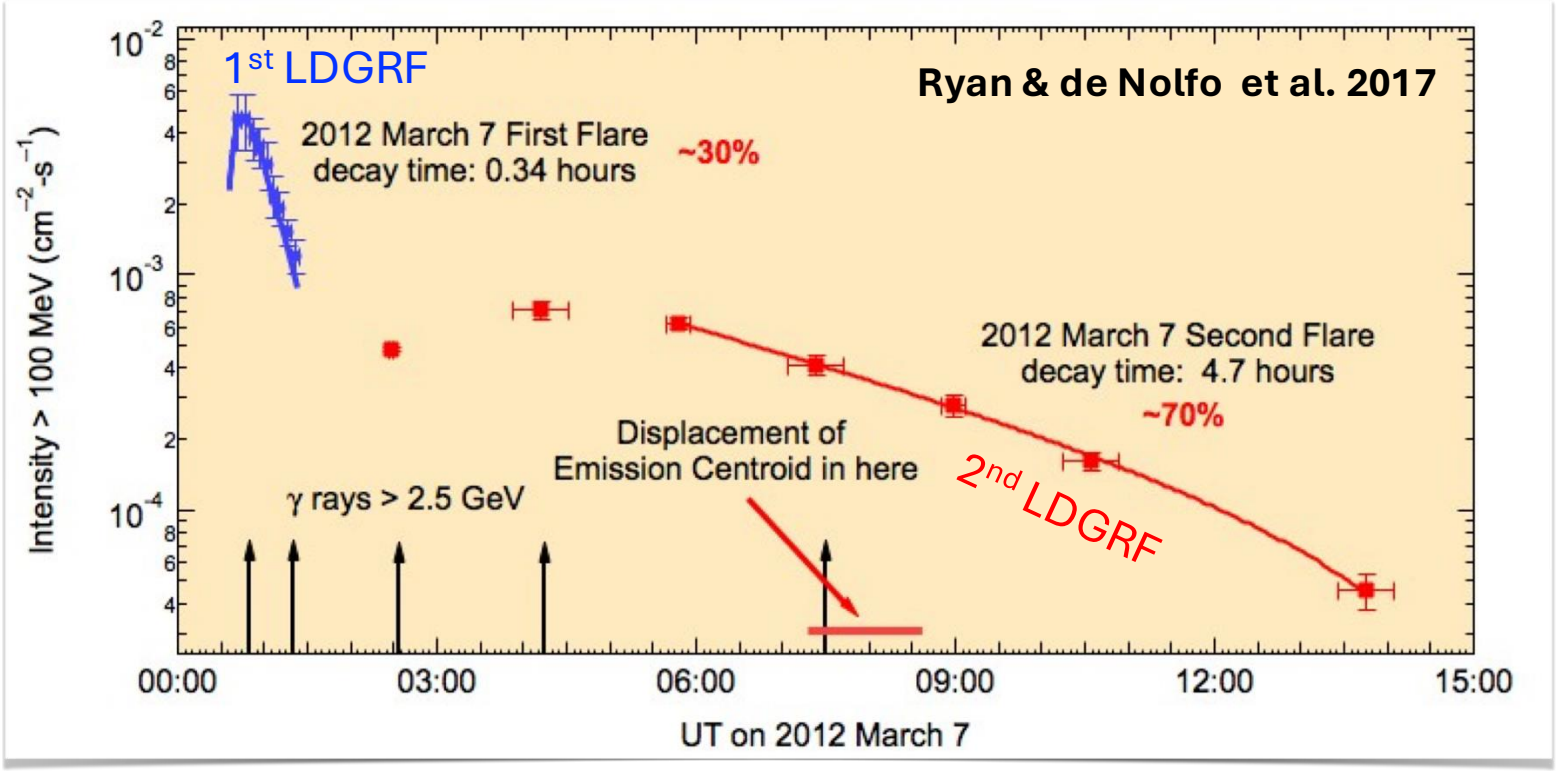


- First flare (X5.4) produced LDGRF consistent with a coronal loop size of ~1 Rs.
- Second flare (X1.3) with L~3 Rs (recall CME is quite far from Sun, and no IP contribution).
- Other combinations of spatial diffusion coefficient and loop lengths are possible, but it is clear that large coronal structures (>$10^5$ km) are necessary for acceleration beyond the pion-production threshold.
- The centroid migration might be due to the different loop contribution and their drift motion.

# The 2017 September 10 LDGRF

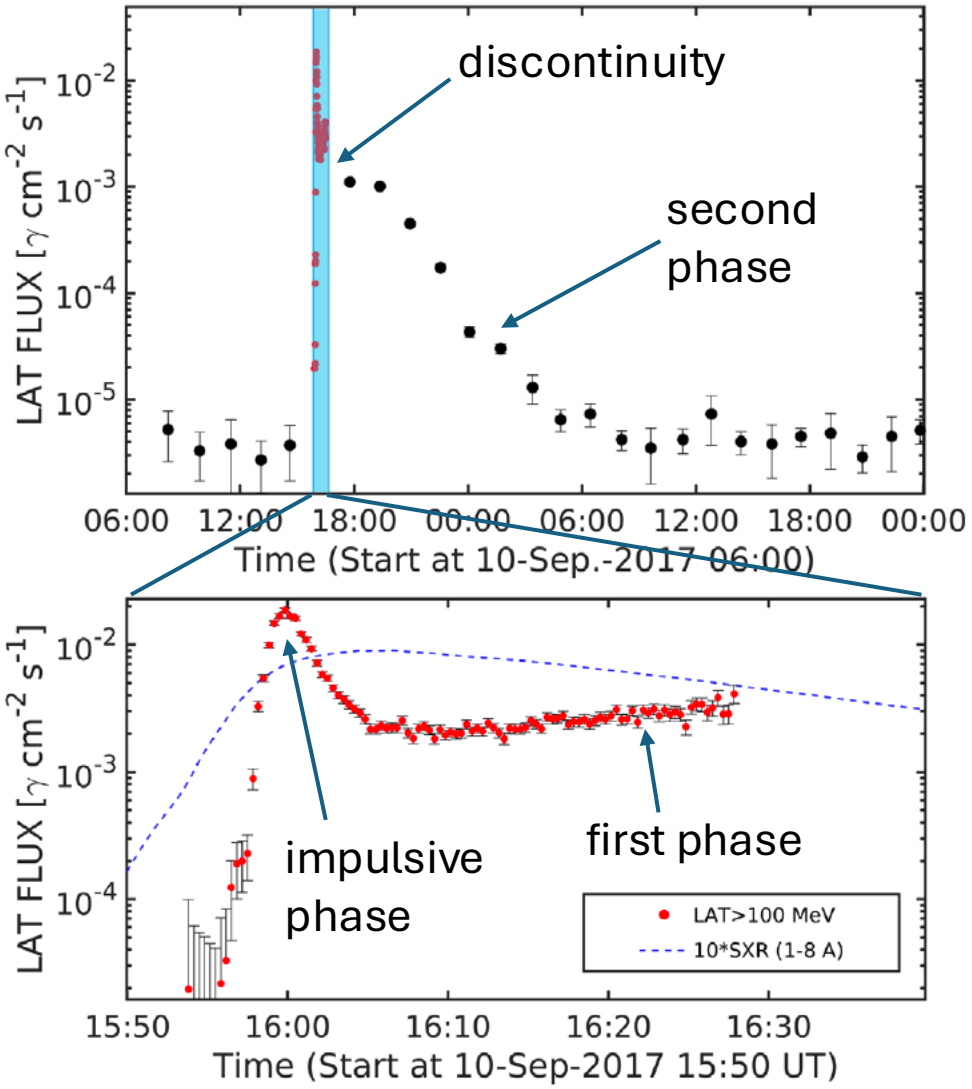


- associated with X8.2 flare from the western limb, very fast (>3000 km/s) CME, and GLE #72.
- Brightest observed by LAT; two-stage >100 MeV LDGRF emission for almost 12 hours (*Omodei et al. 2018*).
- *Kouloumvakos et al. (2020)* found a good correspondence between the temporal evolution of the modeled CME-shock parameters and the γ-ray emission in the first phase,
- concluding that the CME was responsible for both LDGRF/GLE
- The agreement is less good at later times in the event
  - Empirical function used to accounts for shock acceleration and magnetic mirroring
  - They suggested that the discontinuity of a factor ~3 between the two phases was due to a change in the magnetic configuration limiting back-precipitating.
  - However, a strong magnetic turbulence is necessary to account for the LAT centroid location (close to the parent AR).
- According to *Kocharov et al. (2021)*, both the flare and the CME jointly accelerated high-energy protons near the Sun.

# The 2017 September 10 LDGRF

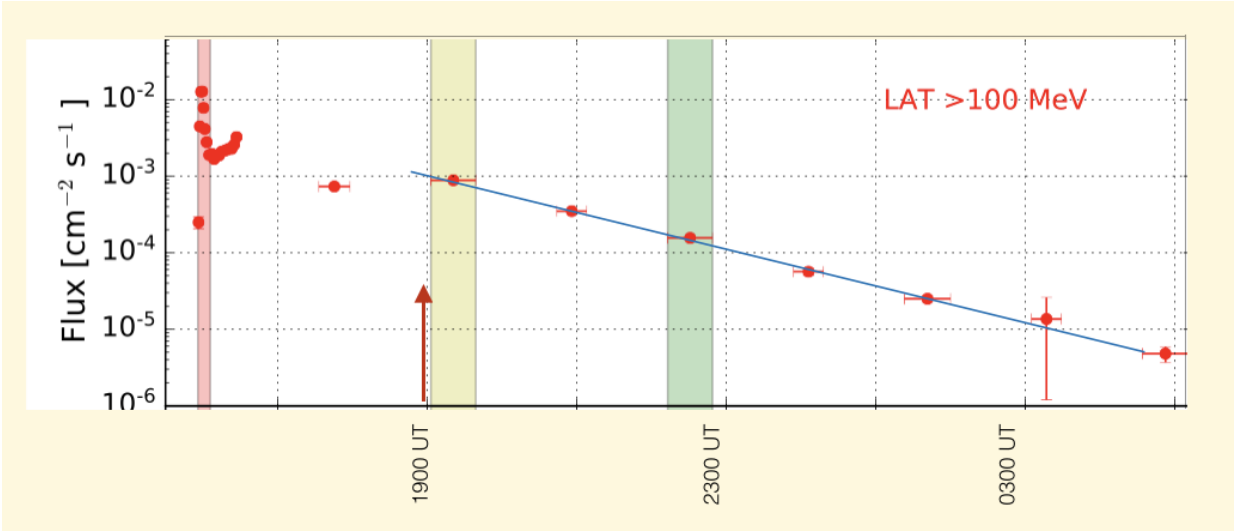


Fit (blue) is smooth exponential decay after 1900 UT, 3 hrs after CME liftoff,
J ~ exp[-(t/6500 s)] +/-20%
Parent proton spectrum softens from -4.3 to -6.0

Ryan *et al.*, 2020

Event Integrated Image at 3.4 Ghz from the *Expanded Owens Valley Solar Array* (EOVSA)

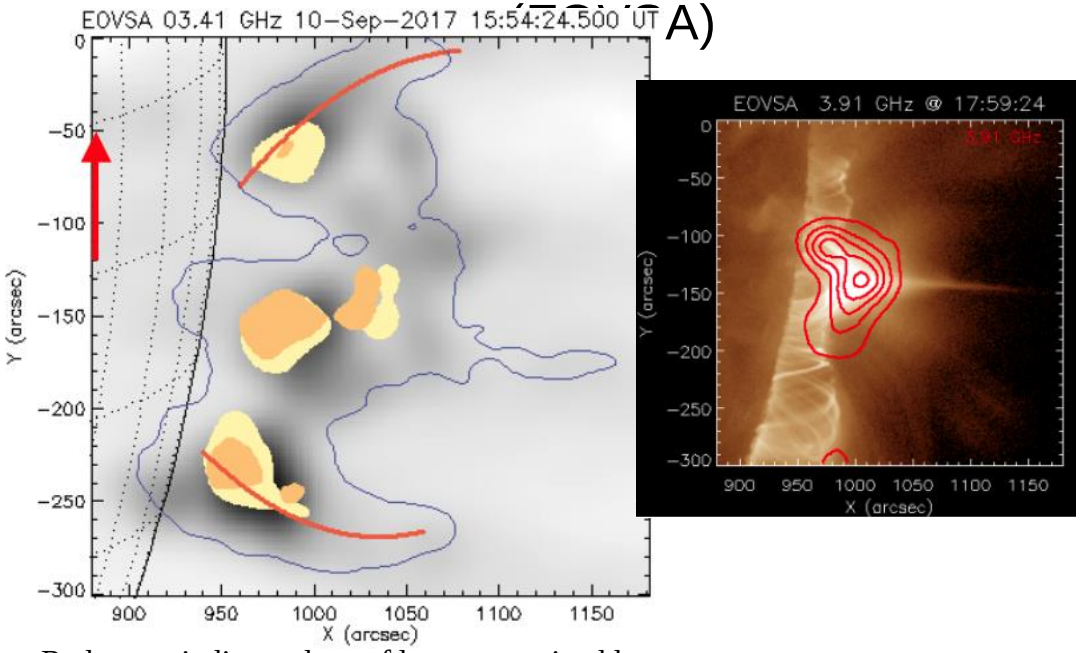


Red curve indicates legs of larger energized loop.

1) complete inner region associated with the lower half of a reconnection event (beneath CME)
2) footpoints of a larger loop with height of 0.4 Rs and L ~ 1.4Rs

# Behind-the-Limb Events

- Protons are accelerated over a spatially-extended region and precipitate down to the atmosphere in the front side of the Sun, away from the original flare site and the HXR emission.
- *Fermi*/LAT observed three LDGRFs associated with BTL sources, 2013 Oct 11, 2014 Jan 6, and 2014 Sept 1 (*Ackermann et al. 2017*), associated with fast CMEs and large SEP events.
- The 2014 Sept 1 was ~40º behind the limb → considered as clear evidence for the CME-shock origin of LDGRFs.
- From these events, it appears that magnetic connectivity is maintained between the CME-driven shock and solar surface enabling particle precipitation (*Plotnikov et al. 2017*).
- Furthermore, it appears that the reconstructed shock fronts become magnetically connected to visible solar surface just before onset of >100 MeV $\gamma$-ray emission while a drop off in intensity is observed as the shock transitioned to quasi-parallel shock geometry (*Jin et al. 2018*).

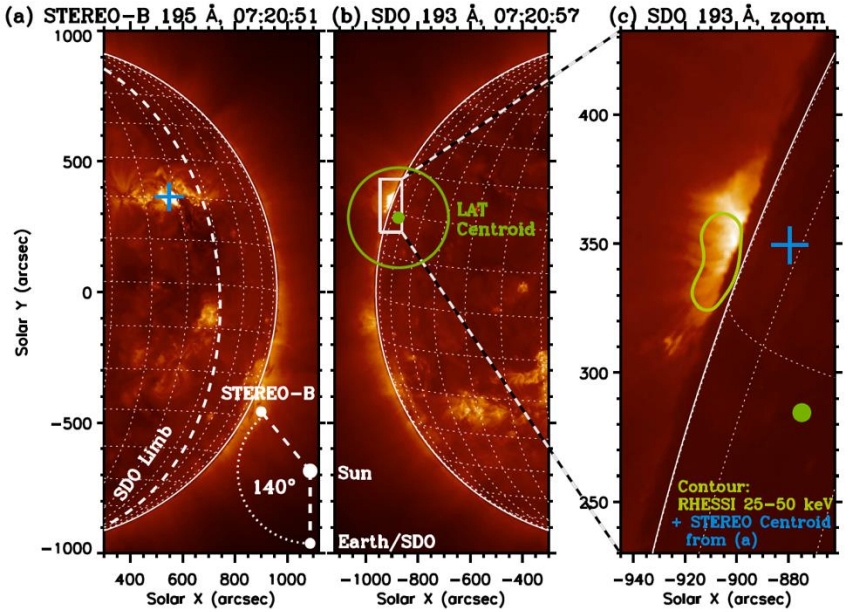


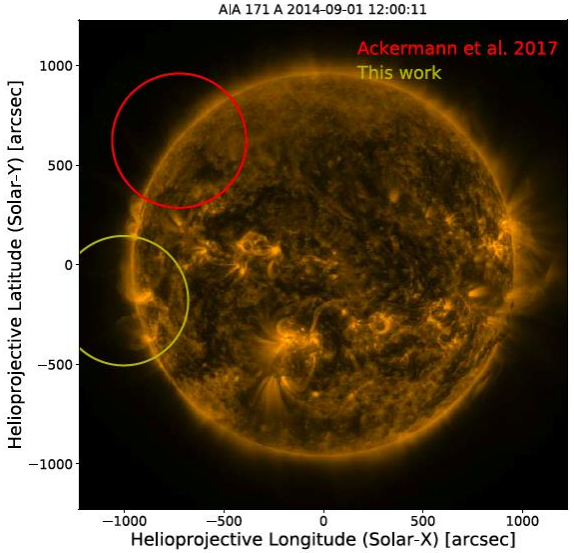

# Behind-the-Limb Events

gyrosynchrotron source according to the NRH data at 432 MHz

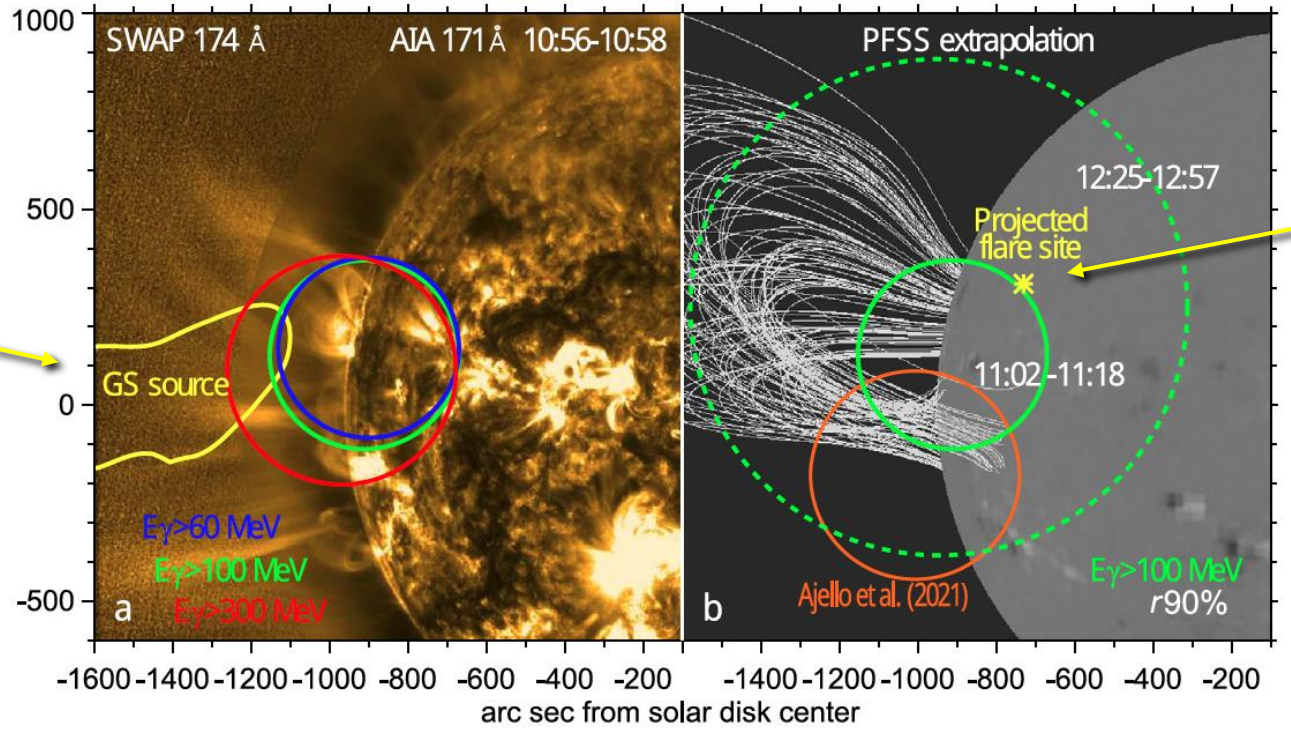


Flaring region behind the limb

- In contrast, *Grechnev et al. (2018)* found the detectable emission during the 2014 Sept 1 event to be consistent with flare-accelerated particles trapped in static long coronal loops and possibly reaccelerated in these loops by a shock wave excited by the initial eruption.
- *Kochanov et al. (2024)* estimated that the (stable) $\gamma$-ray centroid position at two temporal intervals separated by one hour, was close to the bases of long coronal loops connected to the flare site.

# Behind-the-Limb Events

- Very recently, *Pesce-Rollins et al. (2024)* conducted a multi-wavelength investigation of the BTL γ-ray solar flare on 2022 September 29, reporting evidence for flare-accelerated particles in large scale loops.
- The radio spectral imaging based on the Nançay Radioheliograph and ORFEES spectrograph reveal geometries consistent with a magnetic structure that connects the parent AR behind the limb to the visible disk.
- Although not associated with a LDGRF but with an impulsive event, it demonstrates that the >100 MeV γ-ray emission originated from ions accelerated in the parent AR behind the limb can be transported to the visible disk via a large magnetic structure connected to the parent AR behind the limb.

☞ **A CME-driven shock is not a necessary condition for BTL γ-ray flares**

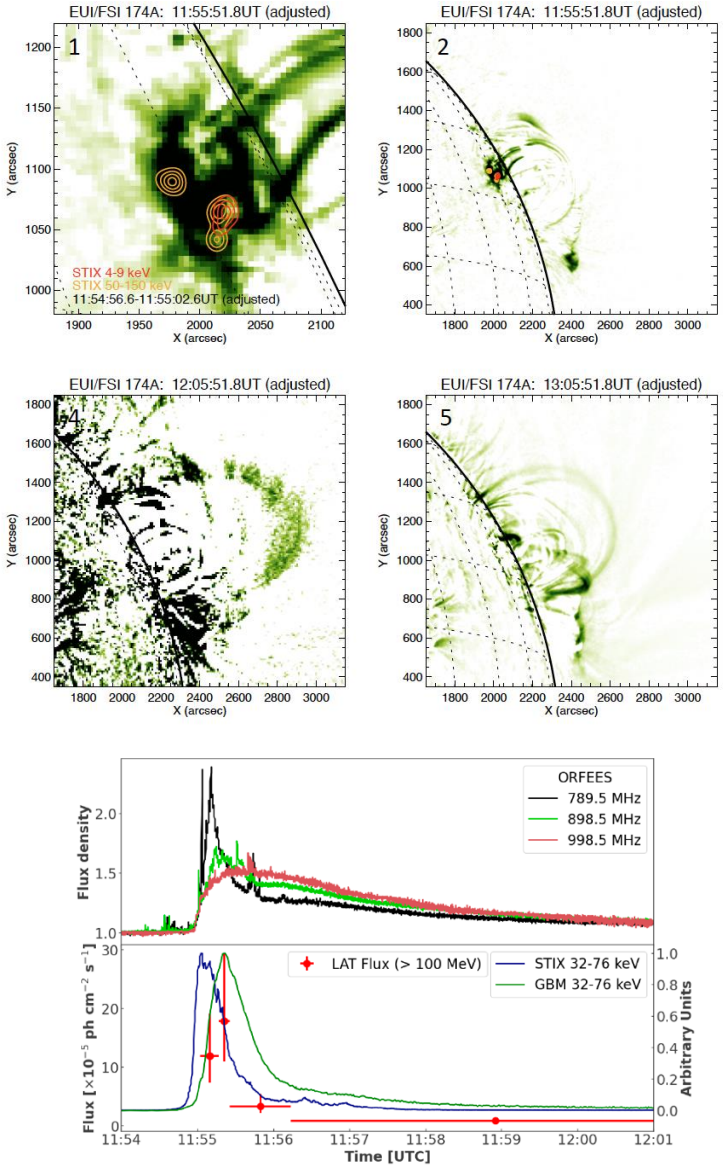

# Relationship between LDGRFs and SEPs

- LDGRFs tend to be associated with relatively fast CMEs, intense type-II radio emission and large SEP events, often with energies typical of ground-level enhancements (GLEs, near-relativistic protons).
- Such statistical correlations have been interpreted as supporting evidence for the CME-shock scenario (e.g., *Winter et al. 2018*, *Gopalswamy et al. 2022*).
- However, the apparent connection with shock-related phenomena is contradicted by noteworthy counterexamples:
  - LDGRFs with CME speeds as low as 830 km/s (vs ~2000 km/s typical of GLEs).
  - LDGRFs with no CME (2012 Oct 23 and Nov 27).
  - Large SEP events with a small γ-ray emission (e.g., 2012 May 17 GLE).
  - Large LDGRFs with small SEP events
    (e.g, 2011 March 7, even accounting for the poor latitudinal connectivity).
  - Observational biases (correlation studies limited to the biggest eruptions).

# Relationship between LDGRFs and SEPs

- As a test of the CME-shock scenario, some authors have investigated the relationship between the inferred particle population producing the high-energy γ-rays and the population of SEPs measured in situ, assuming they are sub-samples of the same population of shock-accelerated particles.
- Specifically, *de Nolfo et al. (2019)* and *Bruno et al. (2023)* used the high-energy observations from PAMELA/GOES and the twin STEREOs, to reconstruct the spatial distribution of 14 large SEP events associated with LDGRFs.
- The total *number of >500 MeV interplanetary protons* $\mathbf{N_{SEP}}$ was then compared with the *number of >500 MeV protons interacting at the Sun* $\mathbf{N_{LDGRF}}$ as inferred by *Share et al. (2018)* based on the *Fermi*-LAT observations.
- The γ-ray source spatial distribution relies on the model by *Murphy et al. (1987)*, accounting for attenuation effects associated with atmospheric absorption. The resulting correction increases with increasing heliocentric angle.
- A similar calculation was more recently carried out by *Ajello et al. (2021)*.

# Relationship between LDGRFs and SEPs

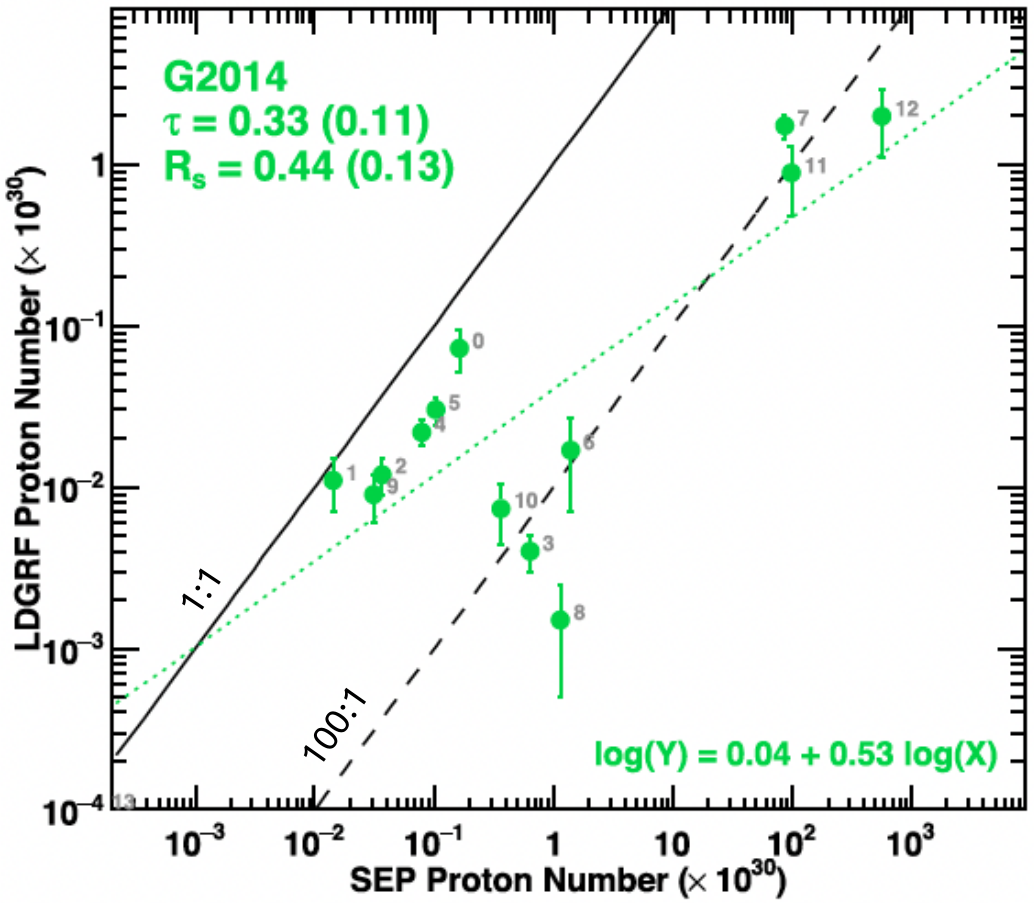


*Interacting vs interplanetary protons*
*(Bruno et al. 2023)*

- The calculation accounts for both longitudinal/latitudinal magnetic connectivity effects on SEP events, as well as longitude-dependent atmospheric absorption of γ rays.
- Even accounting for conservative assumptions related to the γ-ray flare, SEP event, and interplanetary scattering modeling, their statistical relationship was found to be only **poorly/moderately significant**.
- A modified version of this correlation plot was produced by *Gopalswamy et al. (2021)*, based on a double-counting of the aforementioned effects, and some questionable assumptions resulting in a much higher correlation
  - e.g., the γ-ray fluence for the Sept 2014 event was considered to be underestimated by a factor of 560 (implying a similar increase in the precipitation fraction☺)
- In general, though the level of correlation is of interest, it does not provide conclusive evidence for or against a **causal connection** between the two phenomena.

# Relationship between LDGRFs and SEPs

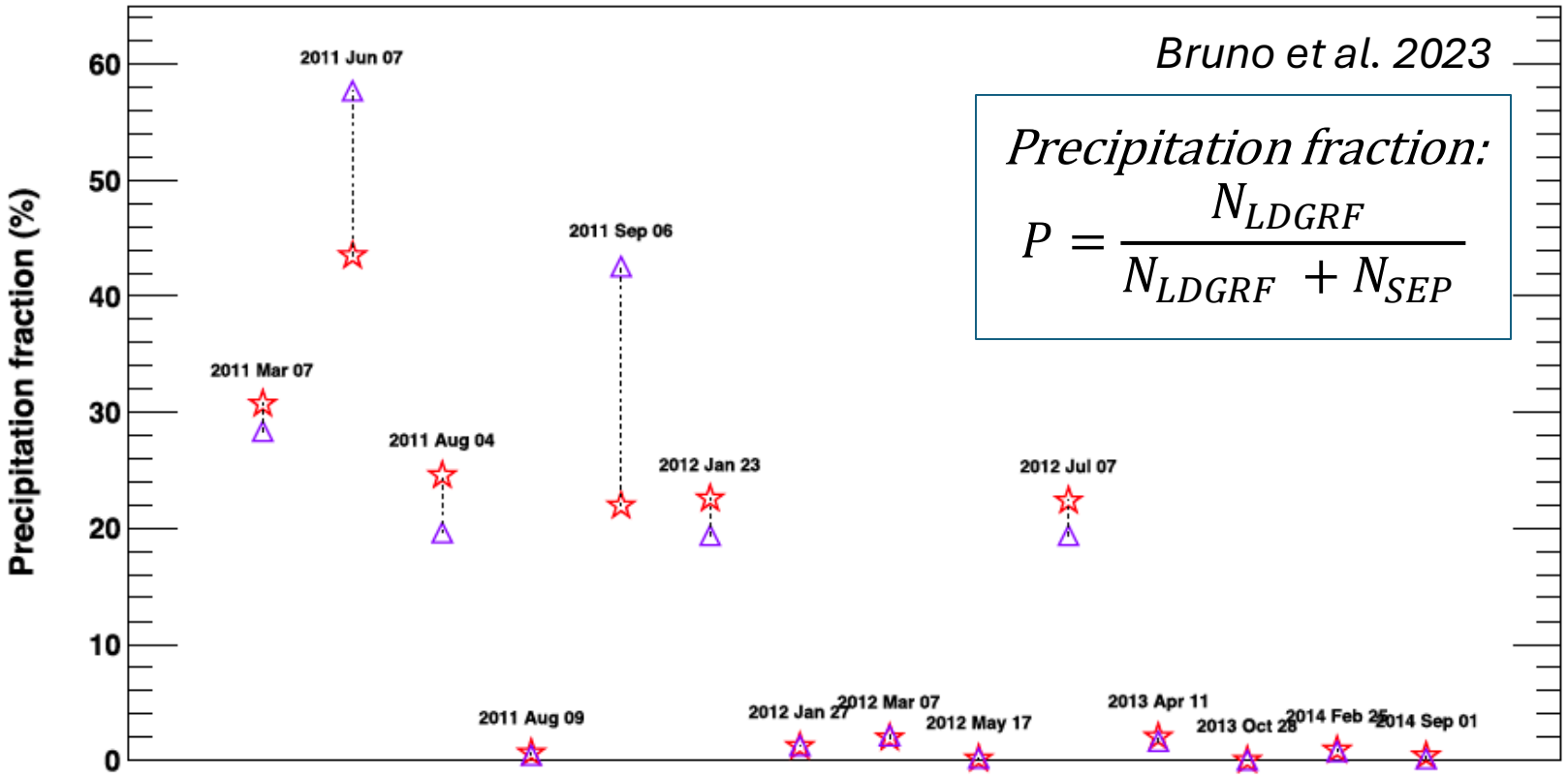


$N_{LDGRF}$ numbers from Share et al. 2018 and Ajello et al. 2021

- On the other hand, the fraction of the shock-accelerated protons required to account for the γ-ray observations is >20%–40% for six of the 14 solar eruptions analyzed.
- Such high values argue against current CME-shock origin models accounting for the **magnetic mirroring.**

# Magnetic Mirroring

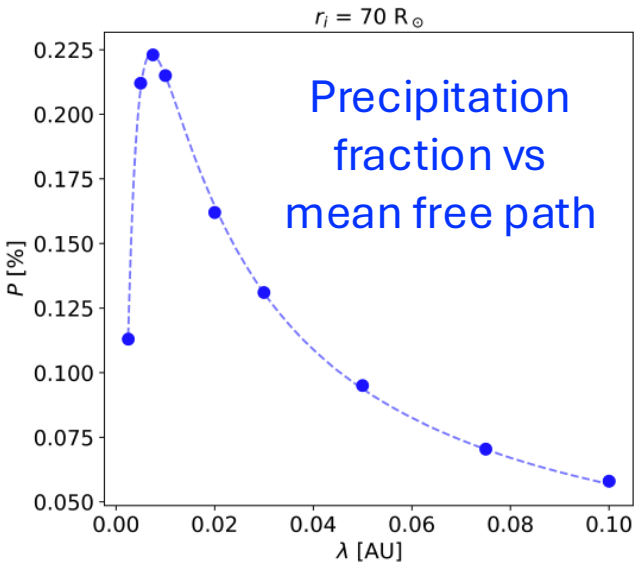


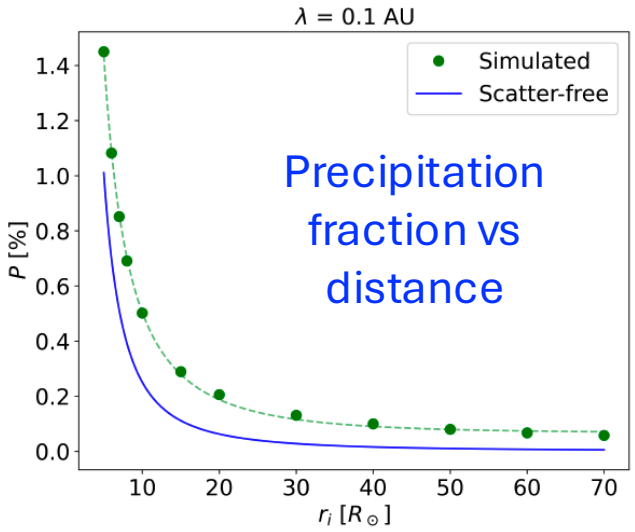


- Particle precipitation to the solar atmosphere is strongly impeded by magnetic mirroring (*Hudson 2018*).
  - The coronal magnetic field tends to focus particles away from the Sun, especially on open field structures.
- Only ions injected nearly parallel to the magnetic field lines in a narrow loss cone can reach a sufficiently dense region of the solar atmosphere to undergo nuclear interactions (*Klein et al. 2018*).
  - Assuming an isotropic particle distribution at the shock, the corresponding fraction amounts to ~1% of the initial population.
- Recently, *Hutchinson et al. (2022)* investigated the mirroring problem extensively using 3D test particle simulations, with varying levels of scattering.
  - While turbulence favors back-precipitation, outward convection with the solar wind dominates at very small mean free paths.
- Back-precipitation efficiency drastically decreases with increasing shock distances, exacerbating the problem for fast CMEs.
- These results suggest that it is not possible to obtain both long-duration γ-ray emission and efficient precipitation within the CME-shock scenario.

# Back-Precipitation from CME-Shocks

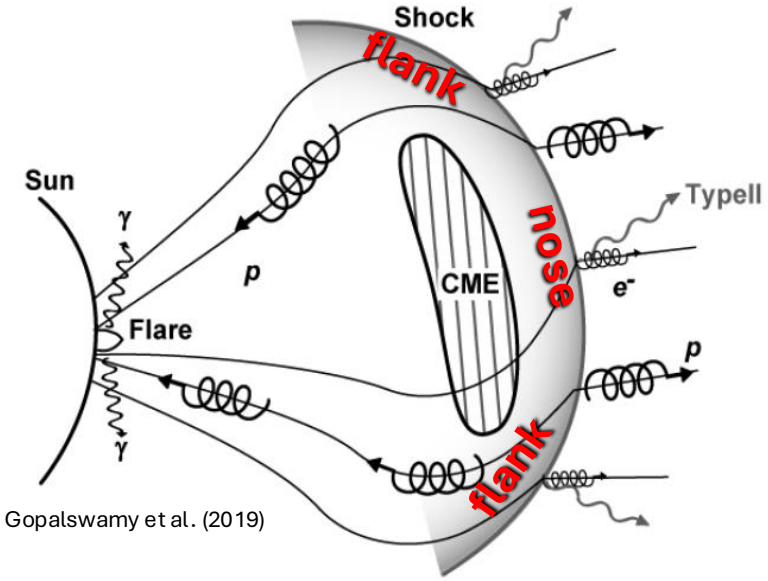

Gopalswamy et al. (2019)

- Higher-energy particles are more efficiently accelerated closer to the Sun (where the coronal magnetic field is strongest) and over a smaller shock region around the "nose" (where the shock is strongest).
- Specifically, the shock-nose region is expected to be the source of the >300 MeV protons producing the LDGRFs
- However, particle propagation throughout the environment behind the shock nose is strongly limited by the sheath and compression-enhanced turbulence, making difficult to achieve an efficient back-precipitation exhibiting a remarkably smooth decay over hours
- Back-precipitation from the flanks is easier, but unable to provide a significant number of high-energy particles (inefficient acceleration)

# Back-precipitation from CME-Shocks

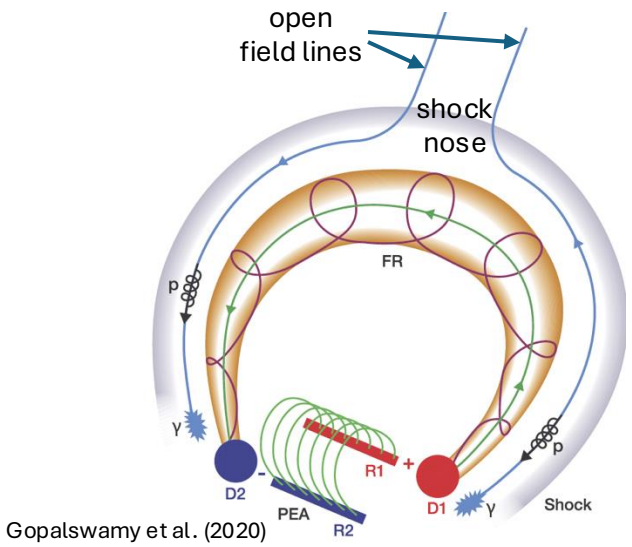

Gopalswamy et al. (2020)

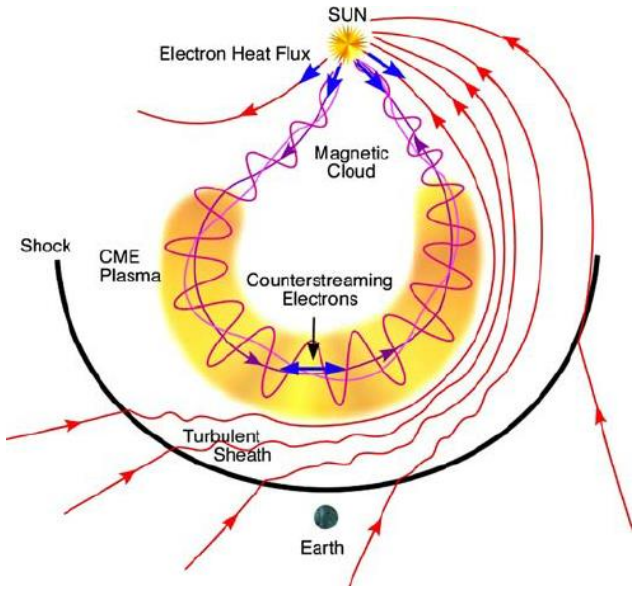


- Another proposed scenario assumes particle transport from the shock nose along open field lines passing through the sheath region.
- Only works close to the Sun, when the shock is still dome-like (top figure).
- In general, it ignores the potential complexity of the open ambient coronal fields that the shock is moving through and unjustifiably assumes that sheath field lines at the nose of the shock map back to the region of the parent AR.
- When the CME is far from the Sun, the shock is more extended, and does not wrap around its body.
- The field-line connection region is expected to be more extended and "diffuse" in longitude, especially as the shock moves away from the Sun where ambient solar-wind field lines forming the sheath are highly unlikely to map back to the source region of the CME (bottom figure).
- And eventually the spiral magnetic field will produce an east-west asymmetry so that the western sheath field lines are connected to the stronger parts of the shock near the nose, while the eastern sheath is connected to the weak eastern flank, so presumably the γ-ray emission will tend to favor western longitudes.

# Correlation with Type-II Radio Emission?

- *Gopalswamy et al. (2018)* reported a significant correlation between the γ-ray and the IP type-II radio emission parameters, based on the sub-sample of largest eruptions.
- However, the correlation is not confirmed when not using only the biggest events, and the LDGRF durations from other authors (*Share et al. 2018*, *Ajello et al. 2021*).
- In general, any connection between the two phenomena is not obvious
  - ✓ Emissions produced by different particles in different regions.
- For the 2012 March 7 LDGRF, the emission ended when the shock was at **0.8 AU**!
- No evidence for continuous acceleration of near-relativistic protons by CME-driven shocks over these long helio-distances
  - ✓ the acceleration efficiency reduces with time as the shock propagates out into the interplanetary space.

❖Whether a magnetic connection to the source AR can be maintained over such distances is very questionable; significant magnetic mirroring.

- Since faster CME-driven shocks typically accelerate particles over larger helio-distances, any apparent relationship with DH radio bursts could be just a reflection of the association of LDGRFs with relatively fast CMEs.

# Coronal-Loop Model (Ryan and Lee)

- Seed ions injected and trapped into large (length $\mathcal{L} \gtrsim 1$ Rs) magnetic bipolar structures (coronal loops) appearing during the gradual phase of two-ribbon flares and CME liftoff via field-line reconnection, creating a system of arches that can persist for several hours.
- Ions are simultaneously accelerated by the 2nd order Fermi process, attaining high energies (100 MeV-1 GeV).
- Wave energy is continually provided from below.
  - For the purpose of accelerating protons, only magnetic turbulence or Alfvén waves are necessary with $\delta B/B \sim 10\%$ (*Ryan et al. 2018*).
- Particle diffuse to ends of the loop and precipitate into the photosphere.
- Because the loop scenario is local and diffusive, it would naturally produce smooth exponential decays, since no sequence of magnetic connects or disconnects would occur, as would be expected for a propagating large-scale feature like a CME.
  - The decay time depends on the turbulence level and loop size: $\tau = \mathcal{L}^2/(\pi^2 k)$
- Delayed onset representing the time required by the ions to exceed the pion production threshold energy.

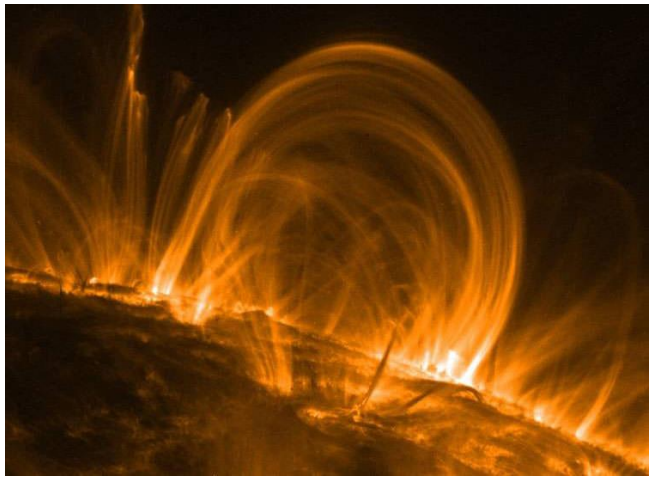

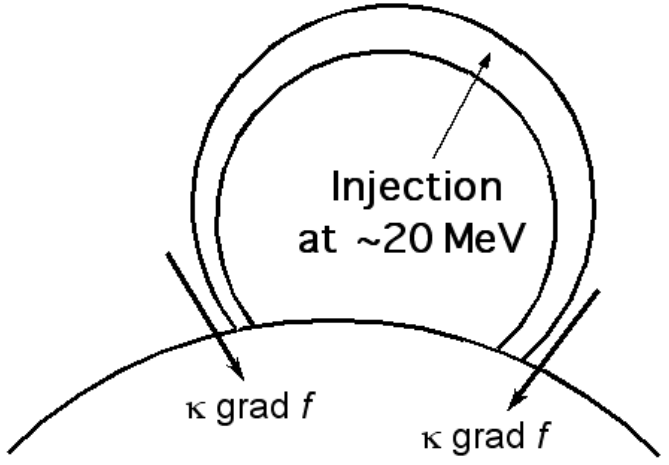


Ryan and Lee, 1991, ApJ 368, 316

# Remaining Challenges

## Shock acceleration

- Mirroring force implies inefficient back-precipitation, while observations suggest high precipitation fractions
- Acceleration efficiency decreases with increasing helio-distances.
- Maintaining magnetic connectivity up to 0.8 AU to produce smooth decay of gamma rays.
- Interacting and interplanetary (SEP) particles typically exhibit spectra with significantly different slopes.
- LDGRFs not accompanied by CMEs.

## Coronal loops

- Large loops quite common, but difficult to visualize.
  - Not filled with hot plasma or enough 100 keV electrons to be visible in soft X-ray or radio emission.
- Uncertainties on the ambient conditions within the loop.
  - With no indicators of loop size, difficult to estimate $\kappa$ from L.
- More theoretical work is necessary to evaluate the appropriate levels of turbulence and wave energy.

# Summary and Conclusions

- The ***Fermi*-LAT** instrument has drastically increased the number (and quality) of solar γ-ray emission observations, significantly improving our understanding of LDGRFs.
- While LDGRFs are known to be caused by high-energy ions interacting with the solar atmosphere, the underlying dominant acceleration process remains controversial.
- The widely-invoked **CME-shock paradigm** is primarily supported by the correlations of LDGRFs with relatively-fast CMEs and large SEP events.
  - However, this could be just a manifestation of the so-called "*big-flare syndrome" (Kahler 1982),* i.e. energetic phenomena are statistically more likely to occur together in large solar eruptions even when there is no specific physical mechanism relating them.
  - Furthermore, an efficient back-precipitation from CME-driven-shock heights is strongly impeded by magnetic mirroring, and by the difficulty of maintaining the magnetic connectivity far from the Sun.
- The **coronal-loop model** represents a natural alternative, explaining both the prolonged/delayed emission and its broad spatial extent, although a more widespread acceptance of this scenario is disfavored by the present difficulty to visualize large-scale coronal loops.
  - Future radio observations will help to place constraints on loop size and the ambient conditions within the loop that will improve the modeling of LDRGFs within this scenario.
  - New particle/turbulence measurements from *Solar Orbiter* and *Parker Solar Probe* close to the Sun, along with solar neutron observations, will provide additional context.
- The "loop vs. shock" debate is far from over and will continue to foster our understanding of SEP acceleration.
- As we approach the peak of **solar cycle 25**, we expect new exciting observations from *Fermi*-LAT, which will possibly add important constraints to this growing picture.

# References


- Bruno *et al.*, 2023, "*Statistical Relationship between Long-duration High-energy Gamma-Ray Emission and Solar Energetic Particles*", *ApJ* 953 187
- Hutchinson *et al.*, 2022, "*Energetic proton back-precipitation onto the solar atmosphere in relation to long-duration gamma-ray flares*", A&A 658 A23
- Ryan *et al.*, 2020, "*Modeling the 2017 September 10 Long Duration Gamma Ray Flare*", *PoS* ICRC2019 1144
- De Nolfo *et al.*, 2019, "*Comparing Long-duration Gamma-Ray Flares and High-energy Solar Energetic Particles*", *ApJ* 879
- Ryan & de Nolfo, 2017, "*The Problematic High-Energy Flares of 2012 March 7*", American Astronomical Society, SPD meeting #48, id.102.0
- Ryan, 2000, "*Long-Duration Solar Gamma-Ray Flares*", *SSRv 93 581*
- Ryan & Lee, 1991, "*On the Transport and Acceleration of Solar Flare Particles in a Coronal Loop*", *ApJ 368 316*

# Blackup Slides

# Solar Neutrons

- Energetic neutrons are produced after impulsive phase, right through high-energy phase.
- Neutron emission belies any delay between impulsive and high-energy phases, i.e., prompt, uninterrupted and continuous acceleration and precipitation.
- Neutrons track the high-energy γ rays
- Unfortunately, very few measurements available…